THE INFLUENCE OF THE ASPECT RATIO ON CONVECTIVE HEAT TRANSFER IN CURVED RETANGULAR DUCTS

Cláudia Regina de Andrade
Edson Luiz Zaparoli
Instituto Tecnológico de Aeronáutica, Departamento de Energia, Pça Marechal Eduardo Gomes, 50, Vila das Acácias, São José dos Campos, SP, Brasil. E-mail: zaparoli@mec.ita.br

Abstract

Convective heat transfer in a curved rectangular duct is numerically studied using a toroidal coordinate system. The laminar flow is considered fully developed and a constant axial temperature gradient is assumed with a peripherally uniform wall temperature condition. The mass conservation, momentum and energy equations are solved by the finite element method. Results showed that the curved tubes have a higher heat transfer rates than equivalent straight ducts due to centrifugal effects. These forces induce secondary flows constituted by two vortices perpendicular to the axial flow direction increasing the momentum and the energy transfer rates. Comparisons made with previously published data for Nusselt number at lower Dean numbers showed good agreement and these results are extended for larger Dean number at this work. The influence of the duct aspect ratio on the Nusselt number and on the friction factor is also analyzed.

Keywords: Curved Duct, Coiled Tube, Dean Number, Finite Element Method

1. INTRODUCTION

Curved ducts are extensively used in chemical reactors, storage tanks, agitated vessels and others heat exchangers. Helical and spirals coils are example of curved tubes. According to Shah and Joshi (1987) curved ducts have a higher heat transfer rates than equivalent straight ducts. It occurs due to secondary flows that increase the momentum and energy exchanges. A large number of works into curved ducts with negligible torsion effects have been completed using a toroidal coordinate system.

The first analytical investigation on flow in a coil tube was performed by Dean (1927) showing that the centrifugal forces induce a secondary flow. These recirculations are represented by two vortices perpendicular to the main axial flow.

Cheng and Akiyama (1970) studied numerically the fully developed laminar forced convection problem in curved rectangular channel. These authors used a finite difference method to solve the governing equations by a stream-function formulation.

The effect of curvature for the Graetz problem in a square duct was investigated by Cheng et al. (1975) for the two basic thermal boundary conditions: constant wall temperature and uniform wall heat flux.

Ghia and Sokhey (1977) analyzed the laminar flow in curved ducts using the three-dimensional parabolized Navier-Stokes equations. For square ducts they found that the Dean's instability phenomena first appeared at Dean number near to 143.

Thomson et al. (1998) investigated the torsion effects in curved ducts of rectangular cross section. They showed that the torsion increases the friction factors and reduces the Nusselt

number when compared with the pure toroidal case. So, they recommended that torsion influence must be minimized to enhance the heat transfer.

At the present work the laminar forced convection in rectangular curved ducts is studied with a constant axial temperature gradient and a peripherally uniform wall temperature condition is assumed. The mass conservation, momentum and energy equations are solved by the finite element method. The influence of the duct aspect ratio on the heat transfer rate and on the friction factor is also analyzed. Results for the Nusselt number were compared with previously published data at lower Dean numbers and showed good agreement. Besides, the Nusselt number and friction factor results are extended for larger Dean number.

2. MATHEMATICAL FORMULATION

Steady-state, laminar and incompressible flow is considered with hydrodynamically and thermally fully developed conditions. The fluid properties are approximately constant, so the energy equation may be decoupled from continuity and momentum equations.

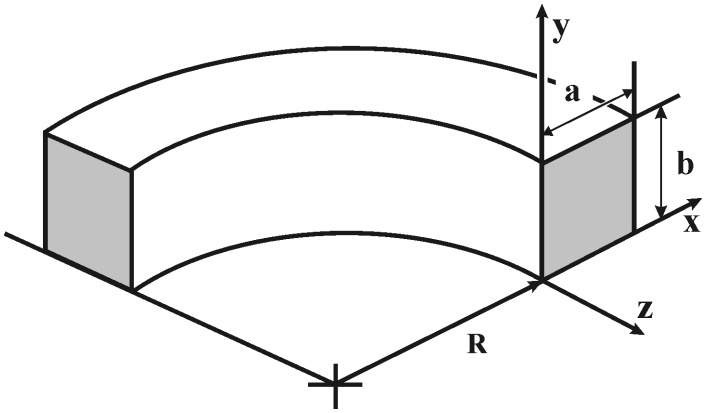

Figure 1. Rectangular curved duct in a toroidal coordinate system

The fully developed flow and the constant axial temperature gradient assumptions result in the following conditions for the velocity and temperature profiles:

$$\frac{\partial u}{\partial z} = \frac{\partial v}{\partial z} = \frac{\partial w}{\partial z} = 0 \;\; ; \;\; \frac{\partial T}{\partial z} = \frac{dT_w}{dz} = \frac{dT_b}{dz} = \text{constant} \tag{1}$$

where:
z is the horizontal axial coordinate (main flow);
w is the velocity component in the z direction;
u and v are the velocity components in the transversal section (secondary flow);
T_w is the wall temperature and T_b is the bulk mean temperature.

The total pressure field P'(x, y, z) is decoupled in an axial contribution and in a parcel corresponding to the transversal direction, as mentioned in Fletcher (1991):

$$P'(x,y,z) = \overline{P}(z) + P(x,y) \tag{2}$$

The governing equations (continuity, energy, x, y and z momentum equations) in the toroidal coordinate system showed in Fig.1 are represented by:

$$\frac{\partial u}{\partial x}+\frac{\partial v}{\partial y}+\frac{u}{R}\left[\frac{1}{1+(x/R)}\right]=0 \tag{3}$$

$$u\frac{\partial u}{\partial x}+v\frac{\partial u}{\partial y}-\frac{w^2}{R(1+x/R)}=-\frac{1}{\rho}\frac{\partial P}{\partial x}+\nu\left[\nabla^2 u+\frac{1}{R(1+x/R)}\frac{\partial u}{\partial x}-\frac{u}{R^2(1+x/R)^2}\right] \tag{4}$$

$$u\frac{\partial v}{\partial x}+v\frac{\partial v}{\partial y}=-\frac{1}{\rho}\frac{\partial P}{\partial y}+\nu\left[\nabla^2 v+\frac{1}{R(1+x/R)}\frac{\partial v}{\partial x}\right] \tag{5}$$

$$u\frac{\partial w}{\partial x}+v\frac{\partial w}{\partial y}+\frac{uw}{R(1+x/R)}=-\frac{1}{(1+x/R)}\frac{1}{\rho}\frac{\partial \overline{P}}{\partial z}+\nu\left[\begin{array}{c}\nabla^2 w+\frac{1}{R(1+x/R)}\frac{\partial w}{\partial x}\\ -\frac{w}{R^2(1+x/R)^2}\end{array}\right] \tag{6}$$

$$u\frac{\partial T}{\partial x}+v\frac{\partial T}{\partial y}+\frac{w}{(1+x/R)}\frac{dT_b}{dz}=\frac{k}{\rho C_p}\left[\nabla^2 T+\frac{1}{R(1+x/R)}\frac{\partial T}{\partial x}\right] \tag{7}$$

where:
z = horizontal axial coordinate (main flow);
w = velocity component in the z direction;
u, v = the velocity components in the transversal section (secondary flow).
R = radius of curvature of the duct;
ρ = fluid density;
ν = fluid kinematic viscosity;
Cp = fluid constant pressure specific heat;
k = fluid thermal conductivity.

Starting from the fluid properties the Prandtl number (Pr) can be defined as:

$$Pr=\frac{\nu\,\rho\,Cp}{k} \tag{8}$$

The boundary conditions for the problem are:

$$u=v=w=0 \quad \text{and} \quad T=T_w \quad \text{at} \begin{cases} x=0,\ \ 0\le y\le b; & x=a,\ \ 0\le y\le b \\ y=0,\ \ 0\le x\le a; & y=b,\ \ 0\le x\le a \end{cases} \tag{9}$$

After numerically determining the axial velocity (w) and the temperature field (T), the average velocity (w_m) and the Reynolds number (Re) were calculated:

$$w_m=\frac{1}{A}\int w\,dA \qquad \text{and} \quad Re=\left(\frac{\rho\,w_m\,D_h}{\mu}\right), \tag{10}$$

where A is the duct cross-section area and D_h is the hydraulic diameter given by:

$$D_h=\frac{2\,a\,b}{(a+b)} \tag{11}$$

The Dean number (*De*) and the duct curvature ratio (*RC*) are calculated as follows:

$$De = Re\sqrt{\frac{D_h}{R}} \quad \text{and} \quad RC = \frac{R}{D_h} \tag{12}$$

The *Nu* (Nusselt number) and *fRe* (friction coefficient and Reynolds number product) are expressed by:

$$Nu = \frac{h\,D_h}{k} \quad \text{and} \quad f\,Re = \left(\frac{-2\,D_h\,(d\overline{P}/dz)}{\rho\,(w_m)^2} \right) Re \tag{13}$$

where the convection coefficient *h* is defined as:

$$h = \frac{q_{wm}}{(T_w - T_b)}, \quad q_{wm} = \frac{(dT_b/dz)\,\rho\,C_p w_m}{(1 + x/R)} \; \frac{(a \cdot b)}{2\,(a+b)} \tag{14}$$

3. NUMERICAL SOLUTION

The laminar forced convection problem was solved numerically using the Galerkin finite element method. An unstructured mesh with triangular elements of six nodes and second-degree interpolation polynomials was applied to the partial differential equations system represented by the equations (3) to (7). The resultant algebraic equations system was solved by an iterative procedure in a coupled (no-segregated) way combining the Conjugated Gradient and Newton-Raphson methods. An adaptive scheme was used with successive mesh refinement in the more intense gradient regions. Fig. 2 presents the computational domain and an intermediary mesh in the solution process for a curved rectangular duct with aspect ratio b/a = 2/3.

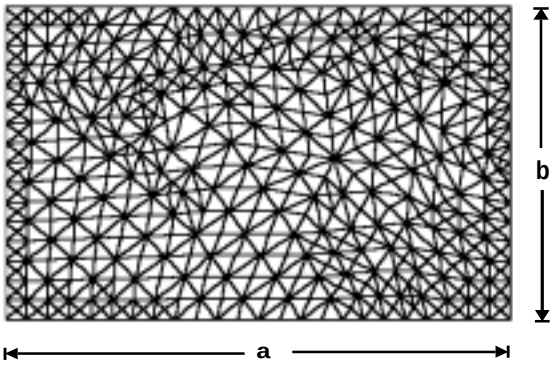

Figure 2. Intermediary mesh in the solution process for a curved rectangular duct

4. RESULTS

At this work the numerical simulations were carried out with *Pr* = 1 (Eq. 8) and for a constant duct curvature ratio R/D_h = 10 (Eq. 12). The numerical results were validated by comparing the Nusselt number and friction factor data (Eq. 13) with the correlation proposed

by Shah and Joshi (1987). This comparison for the curved duct is showed in Fig. 3 and presented a good agreement in the range $80 < De < 140$.

It is verified that the present work provides better results in comparison with the Shah and Joshi (1987) data when the curvature effects are negligible ($De < 80$). For $De > 140$ the difference between the numerical results and the correlation data ever increases. However, as cited in Shah and Joshi (1987), the correlation has a good agreement with the experimental data only for $Pr = 0.7$.

The solid horizontal line in Fig. 3 indicates the straight square duct values presented by Shah and Bhatti (1987). The curved duct (dashed-line) increases the heat transfer and the friction factor in comparison with the straight duct case.

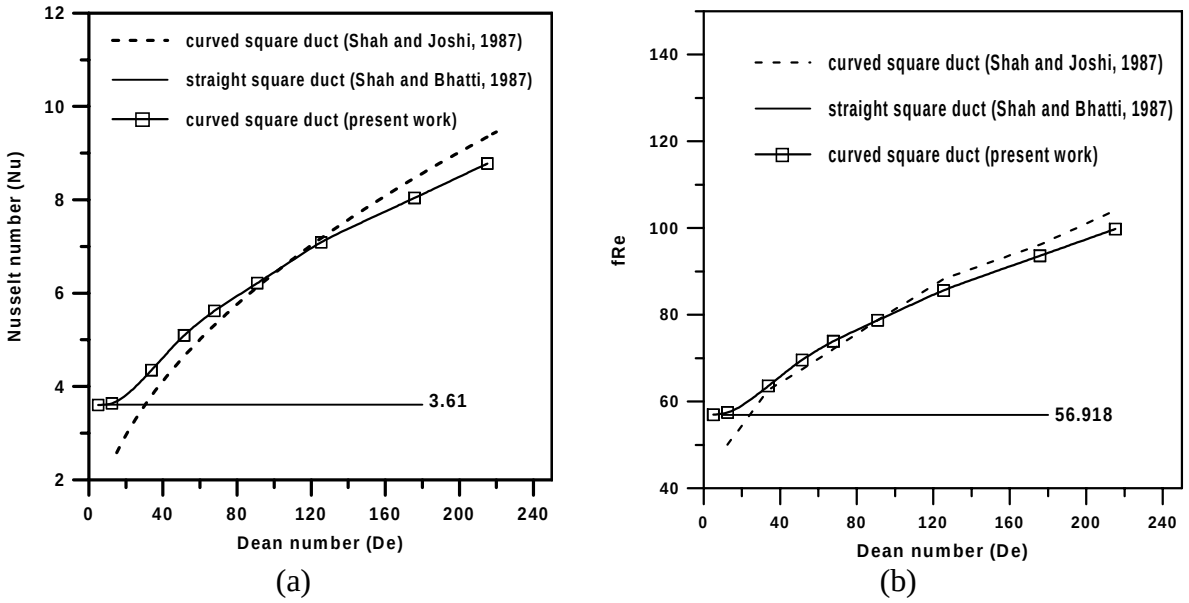

Figure 3. *Nu* and *fRe* results for the curved square duct as a function of the Dean number.

The main axial velocity, the secondary flow vectors plot and the temperature contours obtained for the duct transversal section are shown in Fig. 4 and Fig. 5. The Dean number effect on these distribution patterns for a curved channel with $b/a = 3/2$ is also presented.

It is noted that all contours present symmetric characteristics about the horizontal mid-plane. When *De* number is low (Fig. 4a) the secondary flow is weak. At this case the axial velocity (Fig. 4b) and the temperature distribution also show a symmetric feature about the vertical mid-plane, as the straight duct profiles. As the *De* number increases the secondary flow intensifies and the two-cell cores migrate towards the channel superior and inferior extremes (Fig. 5a).

When $De = 130$, the axial velocity contour becomes more elongated in the vertical direction of the duct cross-section (Fig. 5b) and the curvature effects concentrate the velocity gradients in the right portion of the channel. In Fig. 4c the temperature contours presents only one minimum but in Fig. 5c the distribution shows two minimums (due to a more intense secondary flow) that migrate to the duct extremes as the *De* number increases. The temperature gradient near the external duct wall is intensified due to the secondary flow recirculation cores.

The influence of the duct aspect ratio *b/a* on the curved duct flow is presented in Fig. 6 for $De = 40$. Only the half duct cross-section of the secondary flow vectors plot and the main axial velocity contour are shown.

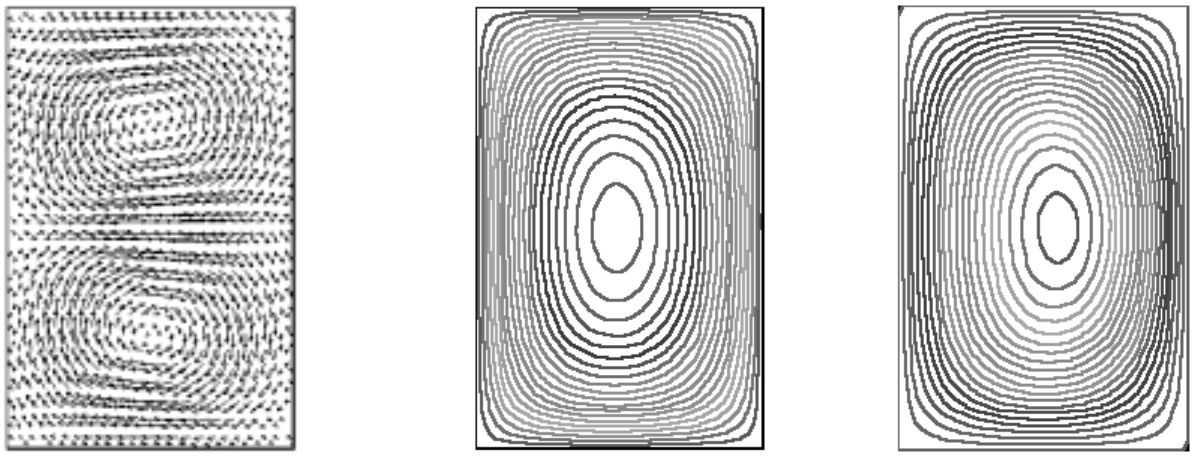

(a) (b) (c)

Figure 4. (a) Secondary flow; (b) axial velocity and (c) temperature contours for *De* = 5

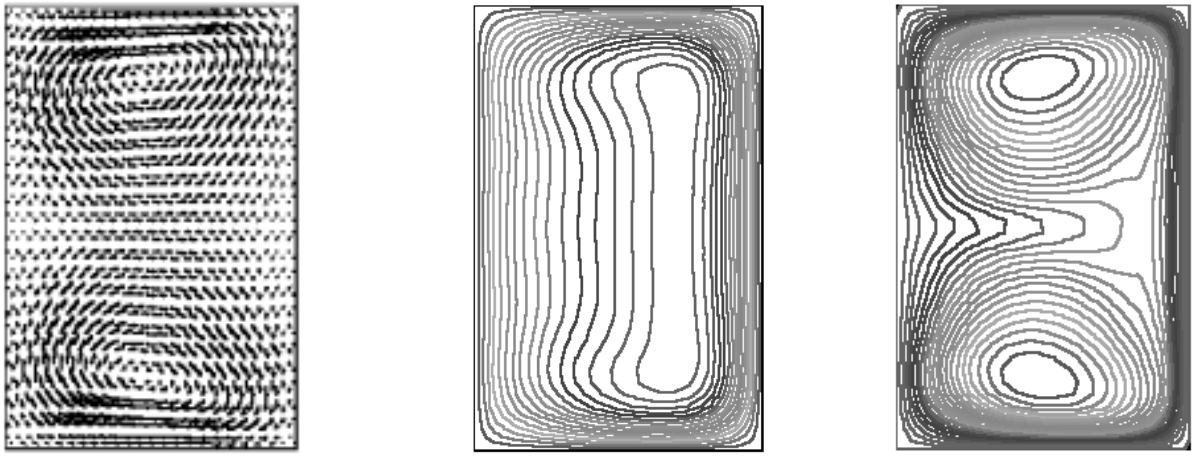

(a) (b) (c)

Figure 5. (a) Secondary flow; (b) axial velocity and (c) temperature contours for *De* = 130

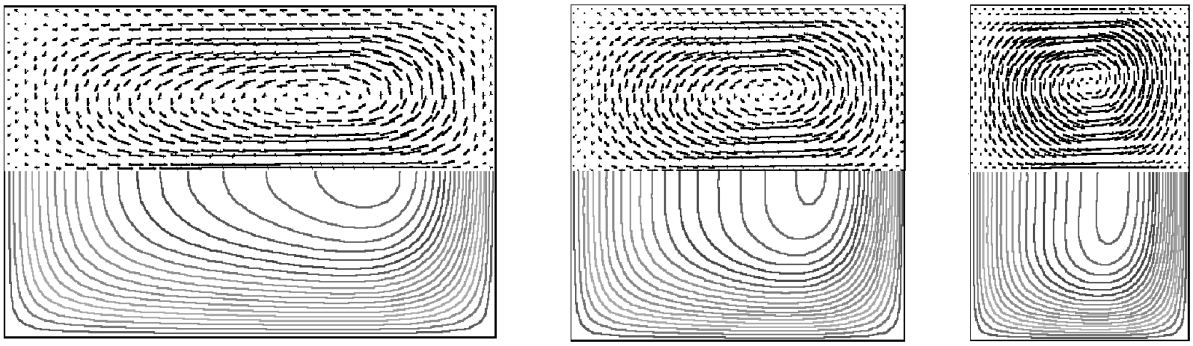

(a) (b) (c)

Figure 6. Secondary flow and axial velocity for (a) *b/a* = 2/3; (b) *b/a* =1 and (c) *b/a* = 3/2

For *b/a* = 2/3 (Fig. 6a) the secondary flow mixing is more intense over the entire duct cross-section but when *b/a* = 3/2 the recirculation cores are displaced to the channel vertical extremes.

The axial velocity profiles at the vertical mid-plane of the duct cross-section for three *b/a* aspect ratios is presented in Fig. 7. It is verified that the inferior and superior boundaries layers are thicker when *b/a* = 2/3. This results that the axial velocity profile at the horizontal mid-plane exhibits also higher values for this *b/a* duct aspect ratio (Fig. 8). Besides the axial velocity distribution maximum values migrates toward the external duct wall when the *b/a* ratio decreases. On the other hand, when the *b/a* ratio is high the secondary flow is more concentrated near the superior and inferior channel extremes (Fig. 6c) with little effect in the central region flow pattern. When *b/a* increases the axial velocity profile tends to a symmetric profile alike the straight parallel plates duct (Fig. 8).

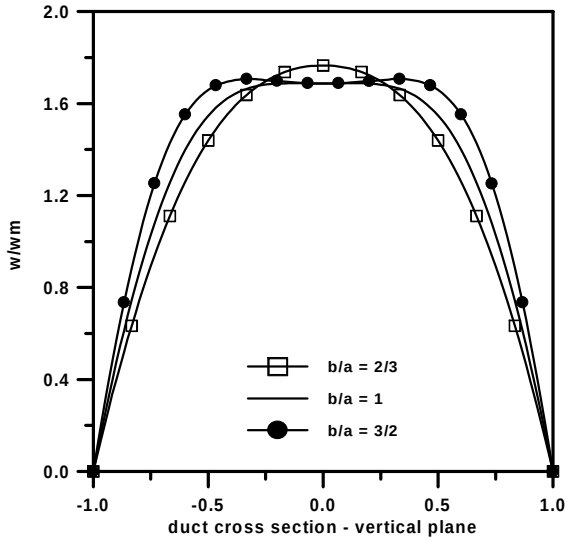

Figure 7. Axial velocity profile at the duct cross-section vertical mid-plane

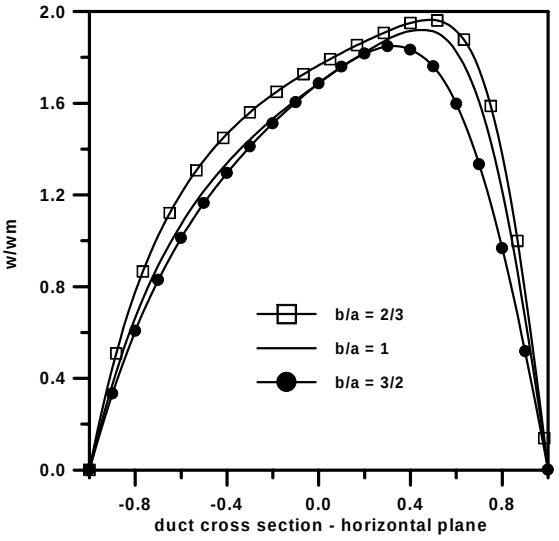

Figure 8. Axial velocity profile at the duct cross-section horizontal mid-plane

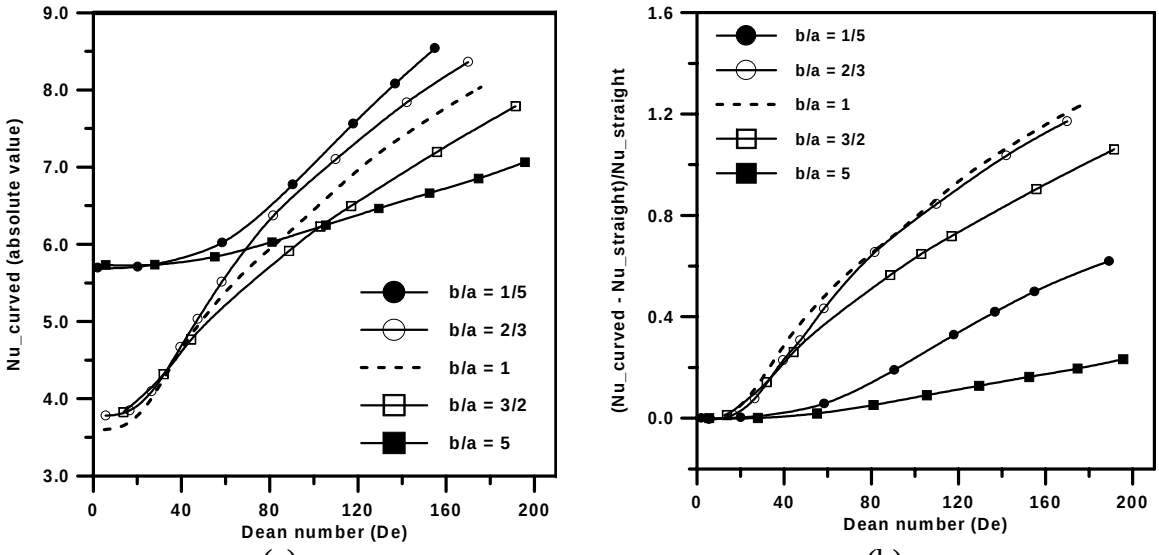

(a) (b)

Figure 9. *Nu* results for the curved rectangular duct as a function of the Dean number for different aspect ratios. (a) absolute value; (b) relative increase

The curved duct Nusselt number results as a function of Dean number for different aspect ratios are presented in Fig. 9a showing that heat transfer rate increases due to the secondary flow. It is verified that when the curvature influence are negligible (low *De* number) the *Nu* results approximates the straight duct value. For small *b/a* ratios the secondary flow mixing effects is more accentuated resulting in higher Nusselt number values. The results shown in Fig. 9a represent an extension of the Thomson et al. (1998) work that provided results in $5 < De < 35$ range.

Fig. 9b presents the curved Nusselt number increases in comparison with the equivalent straight duct, showing that for higher aspect ratios as $b/a = 5$ and $b/a = 1/5$ the curved duct exhibits a little heat transfer increase in comparison with the straight case. Besides, the square channel ($b/a = 1$, dashed-line in Fig 9b) provides the best relative heat transfer enhance.

5. CONCLUSIONS

At this work the fully developed convective heat transfer problem in curved rectangular duct was studied. For all duct aspect ratio analyzed, the Nusselt number results approximate the straight duct value when the Dean number is low. The smaller *b/a* duct aspect ratio provided higher absolute *Nu* value while the curved square channel presented the better relative enhancement.

6. ACKOWLEDGEMENTS

The authors are grateful to FAPESP, which supported this work (grant No. 99/03471-5).

7. REFERENCES

- Cheng, K.C. and Akiyama, M., 1970, "Laminar Forced Convection Heat Transfer in Curved Rectangular Channels", *Int. J. Heat and Mass Transfer*, vol. 13, pp. 471-490.
- Cheng, K.C., Lin, R.C. and Ou, J.W., 1975, "Graetz Problem in Curved Square Channels", *Journal of Heat Transfer*, vol. 97, pp. 244-248.
- Dean, W.R., 1927, "Note on the Motion of Fluid in a Curved Pipe", *Philosophical Magazine*, Series 7, vol. 4, pp. 208-223.
- Fletcher, C.A.J., 1991, "Computational Techniques for Fluid Dynamics", Berlin, Springer.
- Ghia, K.N. and Sokhey, J.S., 1977, "Laminar Incompressible Viscous Flow in Curved Ducts of Regular Cross-Sections", *Journal of Fluids Engineering*, vol. 99, pp. 640-648.
- Shah, R.K. and Bhatti, M.S., 1987, "Laminar Convective Heat Transfer in Ducts", chap. 3 in *Handbook of Single-Phase Convective Heat Transfer"*, S. Kakaç, R.K. Shah and W. Aung, eds., John Wiley & Sons, Inc. N.Y.
- Shah, R.K. and Joshi, S.D., 1987, "Convective Heat Transfer in Curved Ducts", chap. 5 in *Handbook of Single-Phase Convective Heat Transfer"*, S. Kakaç, R.K. Shah and W. Aung, eds., John Wiley & Sons, Inc. N.Y.
- Thomson, D.L., Bayazitoglu, Y. and Meade, A.J., 1998, "Low Dean Number Convective Heat Transfer in Helical Ducts of Rectangular Cross Section", *Journal of Heat Transfer*, vol. 120, pp. 84-91.